Journal of Coordination Chemistry
Publication details, including instructions for authors and subscription information:
http://www.tandfonline.com/loi/gcoo20

Edta-linked 5p-4f trinuclear heterometallic complex: syntheses, X-ray structure and luminescent properties

Juan Shen [a], Bo Jin [a], Qi-Ying Jiang [a], Guo-Qing Zhong [a], Ya-Min Hu [a] & Ji-Chuan Huo [a]

[a] State Key Laboratory Cultivation Base for Nonmetal Composites and Functional Materials, Southwest University of Science and Technology, Mianyang 621010, China

Accepted author version posted online: 06 Jul 2012.Published online: 20 Jul 2012.

To cite this article: Juan Shen, Bo Jin, Qi-Ying Jiang, Guo-Qing Zhong, Ya-Min Hu & Ji-Chuan Huo (2012) Edta-linked 5p-4f trinuclear heterometallic complex: syntheses, X-ray structure and luminescent properties, Journal of Coordination Chemistry, 65:17, 3040-3049, DOI: 10.1080/00958972.2012.709628

To link to this article: http://dx.doi.org/10.1080/00958972.2012.709628

Journal of Coordination Chemistry
Vol. 65, No. 17, 10 September 2012, 3040–3049

Edta-linked 5p–4f trinuclear heterometallic complex: syntheses, X-ray structure and luminescent properties

JUAN SHEN*, BO JIN, QI-YING JIANG, GUO-QING ZHONG, YA-MIN HU and JI-CHUAN HUO

State Key Laboratory Cultivation Base for Nonmetal Composites and Functional Materials, Southwest University of Science and Technology, Mianyang 621010, China

(*Received 7 December 2011; in final form 30 May 2012*)

A new heterometallic antimony–samarium complex, $[Sb_2(edta)_2Sm(H_2O)_4]NO_3 \cdot 3.55H_2O$ (edta = ethylenediaminetetraacetate) (**1**), has been synthesized and characterized by elemental analyses (EA), Fourier transform infrared spectroscopy, thermogravimetry-differential scanning calorimetry, and X-ray crystallography. The X-ray crystal structure analysis reveals that in **1** the bridging carboxylate-O,O′ of $edta^{4-}$ connects samarium(III) and antimony(III) to form 2-D sheets. The 2-D sheets are further linked by bridging carboxylates from adjacent layers, resulting in 3-D coordination polymers. Complex **1** exhibits fluorescence in the solid state at room temperature.

Keywords: Heterometallic complex; Crystal structure; Thermal decomposition; Fluorescence

1. Introduction

Research on the design and synthesis of multifunctional metal-organic frameworks (MOFs) has received attention for fascinating structures and potential applications, such as functional materials in magnetism, non-linear optics, sensors, catalysis, and chemical separations [1–5]. Multidentate ligands such as ethylenediaminetetraacetate (edta) are good choice for constructing heterometallic frameworks due to the existence of different bridging modes. The carboxylates can link 3d and 4f or both 3d and 4f metals [6]. These transition and lanthanide (Ln) metal complexes have interesting molecular properties. A series of complexes with lanthanide and transition metals have been prepared and structurally characterized, such as $MM'(edta) \cdot 6H_2O$ ([MM′] = [MnCo], [MnNi], [MnCu], [CoNi], [CoCu], [NiNi]) with ferrimagnetic chains [7, 8], 3-D coordination polymers with general formula $M''M(M'edta)_2 \cdot 4H_2O$ ([M″MM′] = [CoCoCo], [CoCoNi], [CoNiNi], [ZnNiNi]) [9] and $Ln_2M_3(edta)_3(H_2O)_{11} \cdot 12H_2O$ (Ln=Nd, Gd; M=Mn, Co) [10], and the magnetic properties of lanthanide–transition metal coordination polymers have been studied. However, little work on main group

*Corresponding author. Email: sj-shenjuan@163.com

ISSN 0095-8972 print/ISSN 1029-0389 online
http://dx.doi.org/10.1080/00958972.2012.709628

elements participating in heterometallic complexes has been reported. The 5p element antimony (Sb) is related to potential stereochemical activity of the lone electron pair, giving various structural peculiarities. The synthesis and crystal structures of several antimony(III) complexes with H_4edta, H_3nta, and H_5dtpa have been described [11]. Antimony compounds possess biologic or medicinal properties [12–14], and some complexes with antimony can also treat Leishmaniasis and cancer [15, 16]. To synthesize new antimony complexes with various ligands is interesting for main group element chemistry and for bioinorganic and pharmaceutical chemistry.

Complexes with diaminopolycarboxylates have been an active area of research because carboxylate can coordinate as unidentate, chelating, and bridging bidentate ligands. The aim of this study is to obtain a heterometallic antimony–lanthanide edta complex and investigate its structure, thermal stability, and luminescence. A new 3-D trinuclear antimony–samarium complex, $[Sb_2(edta)_2Sm(H_2O)_4]NO_3 \cdot 3.55H_2O$ (**1**), is synthesized and characterized by elemental analyses (EA), Fourier transform infrared spectroscopy (FT-IR), single crystal X-ray diffraction, thermogravimetry-differential scanning calorimetry (TG-DSC), and the luminescence of **1** were also investigated.

2. Experimental

2.1. *Synthesis of H[Sb(edta)]·H_2O*

Totally 5 mmol of H_4edta was dissolved in 100 mL of hot distilled water, and then 3 mmol of antimonous oxide was added to it. After stirring the solution at 95°C for 6 h, the solution was filtered while hot and the clear and colorless filtrate concentrated. While slowly cooling the filtrate, white crystals were obtained. Anal. Calcd for $C_{10}H_{15}O_9N_2Sb$ (%): C, 27.99; H, 3.53; N, 6.53. Found (%): C, 27.78; H, 3.46; N, 6.42. IR spectrum (cm^{-1}): 3423(w), 3017(m), 1691(s), 1445(m), 1418(s), 1393(s), 1088(w).

2.2. *Synthesis of 1*

Totally 1 mmol of $H[Sb(edta)] \cdot H_2O$ was dissolved in 50 mL of distilled water at 95°C. 1 mmol of NH_4HCO_3 was added to the solution with constant stirring for 30 min. Then, 1 mmol of $Sm(NO_3)_3 \cdot 6H_2O$ was added to the reaction medium. After stirring for 2 h at 50°C, the mixture became almost transparent and was then filtered. Primrose block crystals were obtained after a week, yielding 62% based on the content of Sb. The products are stable in air and soluble in hot water, and not soluble in most common organic solvents, such as anhydrous ethanol and acetone. Anal. Calcd for $C_{20}H_{39.11}N_5O_{26.55}Sb_2Sm$ (%): C, 20.56; H, 3.37; N, 5.99. Found (%): C, 20.75; H, 3.45; N, 6.08. IR spectrum (cm^{-1}): 3413(m), 2952(w), 1664(s), 1587(s), 1448(w), 1407(w), 1384(s), 1082(m).

2.3. *Physical measurements*

EA were performed with a Euro EA 3000 elemental analyzer. IR (KBr pellet) spectra were recorded (400–4000 cm^{-1} region) on a Nicolet-6700 FT-IR spectrometer.

Table 1. Crystal data and structure refinement for **1**.

Empirical formula	$C_{20}H_{39.11}N_5O_{26.55}Sb_2Sm$
Formula weight	1168.38
Temperature (K)	103(2)
Wavelength (Å)	0.71073
Crystal system	Monoclinic
Space group	*P*n
Unit cell dimensions (Å, °)	
a	7.2094(12)
b	22.652(4)
c	10.6553(19)
α	90
β	90.554(2)
γ	90
Volume (Å^3), *Z*	1740.0(5), 2
Calculated density (Mg m^{-3})	2.230
Absorption coefficient (mm^{-1})	3.317
F(000)	1141
Crystal size (mm^3)	$0.40 \times 0.32 \times 0.18$
θ range for data collection (°)	3.31–27.49
Limiting indices	$-9 \le h \le 9$, $-29 \le k \le 28$, $-13 \le l \le 13$
Reflections collected	15,695
Independent reflection	7588 ($R_{int} = 0.0303$)
Completeness to $\theta = 27.49$ (%)	99.5
Max. and min. transmission	0.5867 and 0.3505
Data/restraints/parameters	7588/21/531
Goodness-of-fit on F^2	0.999
Final *R* indices [$I > 2\sigma(I)$]	$R_1 = 0.0288$, $wR_2 = 0.0623$
R indices (all data)	$R_1 = 0.0313$, $wR_2 = 0.0634$

The thermal-induced weight loss of **1** was measured by a thermogravimetric analyzer (SDT Q600 TGA instrument, TA Instruments, United States) using an alumina pan as sample holder. The measurement was recorded from 30°C to 1100°C at 10°C min^{-1} heating rate under air. Fluorescence spectra were recorded on a FL-4500 spectrofluorophotometer (SHIMADZU Co., Japan) for the solid-state samples.

2.4. *X-ray crystallography*

Appropriate crystals were cut from larger ones and mounted on a Bruker Smart 1000 CCD diffractometer with graphite monochromated Mo-Kα radiation ($\lambda = 0.71073$ Å). The data were collected at 103(2) K using multi-scan modes. SHELXS-97 and SHELXL-97 were used for structure determination and refinement [17, 18]. The structure was solved by direct methods, and all non-hydrogen atoms were obtained from the difference Fourier map and subjected to anisotropic refinement by full-matrix least-squares on F^2. All non-hydrogen atoms were refined anistropically. All hydrogen atoms based on carbon were generated theoretically, while other hydrogen atoms were not located. The details of crystal data collection and refinement parameters for **1** are listed in table 1. Selected bond lengths and angles are listed in table 2.

Table 2. Selected bond lengths (Å) and angles (°) for **1**.

Sb(1)–O(7)	2.119(4)	Sb(1)–O(1)	2.206(4)	Sb(1)–O(3)	2.507(4)
Sb(1)–O(5)	2.516(4)	Sb(1)–N(1)	2.313(4)	Sb(1)–N(2)	2.321(5)
Sb(2)–O(11)	2.133(4)	Sb(2)–O(13)	2.215(4)	Sb(2)–O(15)	2.466(4)
Sb(2)–O(9)	2.517(4)	Sb(2)–N(3)	2.308(5)	Sb(2)–N(4)	2.319(4)
Sm(1)–O(4)#1	2.359(4)	Sm(1)–O(6)	2.361(4)	Sm(1)–O(10)	2.360(4)
Sm(1)–O(16)#2	2.377(4)	Sm(1)–O(17)	2.500(4)	Sm(1)–O(18)	2.453(4)
Sm(1)–O(19)	2.452(4)	Sm(1)–O(20)	2.482(4)		
O(1)–Sb(1)–N(1)	73.33(15)	O(1)–Sb(1)–N(2)	76.79(16)	O(1)–Sb(1)–O(3)	109.17(14)
O(1)–Sb(1)–O(5)	89.60(14)	O(3)–Sb(1)–O(5)	147.82(12)	O(7)–Sb(1)–O(1)	144.77(14)
O(7)–Sb(1)–N(1)	79.52(16)	O(7)–Sb(1)–N(2)	75.68(15)	O(7)–Sb(1)–O(3)	80.20(13)
O(7)–Sb(1)–O(5)	99.64(15)	N(1)–Sb(1)–N(2)	77.38(16)	N(1)–Sb(1)–O(3)	68.34(14)
N(2)–Sb(1)–O(3)	141.00(14)	N(2)–Sb(1)–O(5)	67.44(14)	O(11)–Sb(2)–O(13)	144.63(15)
O(11)–Sb(2)–N(3)	75.45(15)	O(11)–Sb(2)–N(4)	78.82(15)	O(11)–Sb(2)–O(9)	100.47(14)
O(11)–Sb(2)–O(15)	80.04(13)	O(13)–Sb(2)–N(3)	77.99(16)	O(13)–Sb(2)–N(4)	72.85(15)
O(13)–Sb(2)–O(9)	90.44(14)	O(13)–Sb(2)–O(15)	107.86(14)	O(15)–Sb(2)–O(9)	147.76(12)
N(3)–Sb(2)–O(15)	141.01(13)	N(3)–Sb(2)–N(4)	77.31(16)	N(3)–Sb(2)–O(9)	67.59(14)
N(4)–Sb(2)–O(15)	68.45(14)	N(4)–Sb(2)–O(9)	143.66(14)	O(4)#1–Sm(1)–O(18)	74.82(14)
O(4)#1–Sm(1)–O(10)	104.71(13)	O(4)#1–Sm(1)–O(6)	83.97(14)	O(4)#1–Sm(1)–O(16)#2	149.19(13)
O(4)#1–Sm(1)–O(19)	83.63(14)	O(4)#1–Sm(1)–O(20)	140.07(13)	O(4)#1–Sm(1)–O(17)	70.41(13)
O(6)–Sm(1)–O(16)#2	105.38(13)	O(6)–Sm(1)–O(20)	77.47(14)	O(6)–Sm(1)–O(19)	72.19(14)
O(6)–Sm(1)–O(18)	139.23(14)	O(6)–Sm(1)–O(17)	75.69(13)	O(10)–Sm(1)–O(18)	72.58(13)
O(10)–Sm(1)–O(16)#2	83.25(13)	O(10)–Sm(1)–O(20)	76.23(14)	O(10)–Sm(1)–O(6)	147.60(14)
O(10)–Sm(1)–O(19)	139.00(14)	O(10)–Sm(1)–O(17)	78.04(13)	O(16)#2–Sm(1)–O(18)	79.56(14)
O(16)#2–Sm(1)–O(20)	70.56(13)	O(16)#2–Sm(1)–O(19)	71.99(14)	O(16)#2–Sm(1)–O(17)	140.08(13)
O(18)–Sm(1)–O(17)	126.17(13)	O(18)–Sm(1)–O(20)	138.79(14)	O(19)–Sm(1)–O(20)	122.37(15)
O(19)–Sm(1)–O(18)	71.17(14)	O(19)–Sm(1)–O(17)	140.40(13)	O(20)–Sm(1)–O(17)	70.86(12)

Symmetry transformations used to generate equivalent atoms: #1 $x+1/2, -y, z+1/2$; #2 $x-1/2, -y+1, z+1/2$.

3. Results and discussion

3.1. *Molecular and crystal structure*

The molecular structure of **1** is depicted in figure 1. The asymmetric unit contains two antimony ions, one samarium, two crystallographically unique $edta^{4-}$ ligands, coordinated water and lattice water molecules. Each $edta^{4-}$ consists of chelating carboxylate and bidentate syn-anti carboxylate bridges over a samarium and two antimony ions. The $edta^{4-}$ coordinates to Sb(III) hexidentate through four oxygen atoms of the carboxylates and two nitrogen atoms, forming four five-membered chelate rings. Selected bond lengths and angles are given in table 2. The sum of the equatorial angles O(3)–Sb(1)–O(5), N(1)–Sb(1)–N(2), N(1)–Sb(1)–O(3), and N(2)–Sb(1)–O(5) is 360.98°, which shows that O(3), O(5), N(1), N(2), and Sb are located in one plane. O(3)–Sb–O(5) of 147.82(12)° is almost twice larger than N(1)–Sb–O(3) (68.34(14)°), N(1)–Sb–N(2) (77.38(16)°), or N(2)–Sb–O(5) (67.44(14)°), which may be caused by the existence of a lone electron pair at the equatorial position. Therefore, the coordination polyhedron of antimony is a ψ-pentagonal bipyramidal environment [11]. In table 2, Sb–O and Sb–N bond lengths are 2.119(4)–517(4) and 2.308(5)–2.321(5) Å, respectively, in the normal range of those observed in other Sb(III)–edta complexes [19, 20]. In **1**, the bidentate chelating bond distances (Sb(1)–O(5) 2.516(4) and Sb(1)–O(3) 2.507(4) Å) are longer than monodentate bond distances (Sb(1)–O(1) 2.206(4) and Sb(1)–O(7) 2.119(4) Å). All O–Sb–O, N–Sb–N, and O–Sb–N bond angles fall in the range of

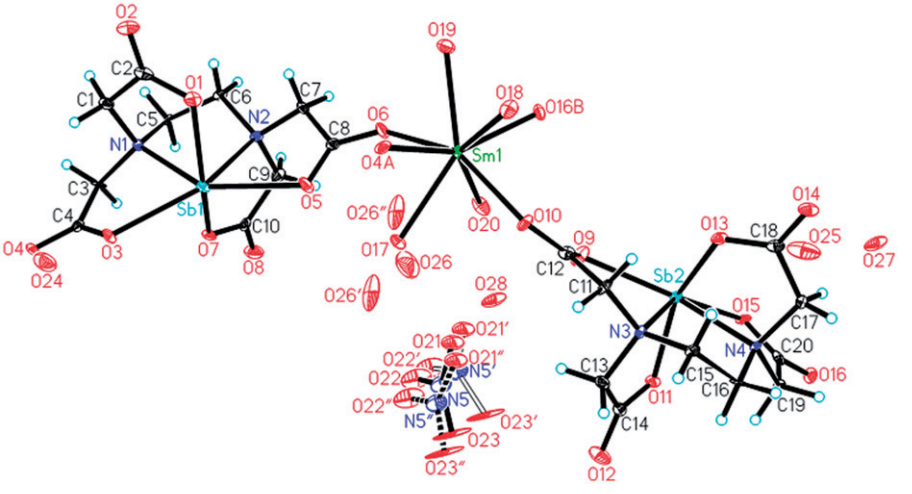

Figure 1. The asymmetric unit of **1** with atom-numbering scheme. Displacement ellipsoids are drawn at the 50% probability level. (Symmetry transformations used to generate equivalent atoms: A = $x+1/2$, $-y$, $z+1/2$; B = $x-1/2$, $-y+1$, I + 1/2).

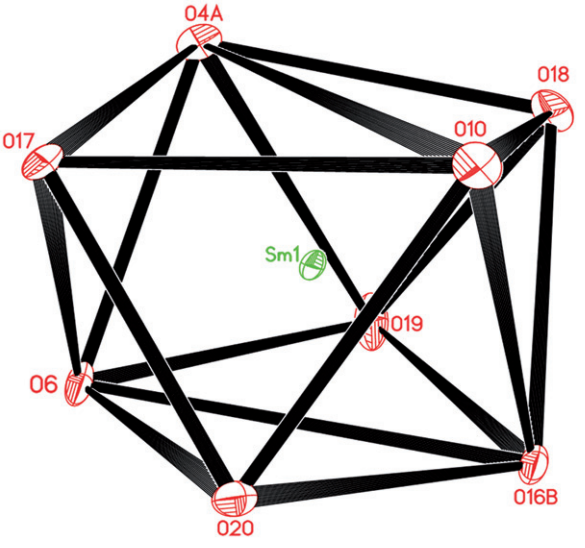

Figure 2. Coordination polyhedron around Sm(1) in **1** (Symmetry transformations used to generate equivalent atoms: A = $x+1/2$, $-y$, $z+1/2$; B = $x-1/2$, $-y+1$, I + 1/2).

80.20(13)–147.82(12)°, 77.31(16)–77.38(16)°, and 67.44(14)–143.66(14)°, respectively, similar to those in the related Sb–edta complexes [21].

As shown in figure 2, the coordination polyhedron around each samarium is a distorted square antiprism with four sites occupied by four oxygen atoms from coordinated water molecules (O(17), O(18), O(19), and O(20)) and four sites occupied

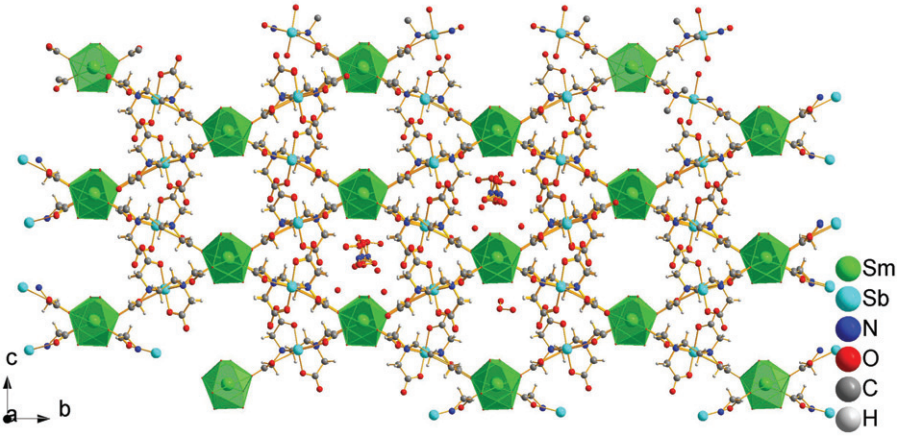

Figure 3. A 2-D network representation of **1** along the *a*-axis.

by four edta^{4-} ligands (O(4A), O(6), O(10), and O(16B)). O(4A), O(18), O(10), O(17) and O(6), O(20), O(16B), O(19) form upper and lower square planes, respectively. The Sm–O distances range from 2.359(4) to 2.500(4) Å (average value = 2.408(4) Å) (table 2). The O–Sm–O bond angles are 70.41(3)–149.19(13)°, similar to those in the related Sm(III) complexes [21–23]. Generally, lanthanide(III) metal complexes with aminopolycarboxylic acids adopt eight-, nine-, or 10-coordinate structures. Their structures and coordination numbers largely depend on ionic radius, electron configuration, nature of counter cation(s), as well as the shape of ligands [24]. Sm(III), with relatively large ionic radius and $4f^5$ electron configuration, commonly forms nine-coordinate structures with most aminopolycarboxylic acids [25]. The present Sm(III) complex has eight as the coordination number, as reported for lanthanide(III) complexes [26].

All H_4edta are deprotonated and coordinate Sb(III) and Sm(III). Carboxylate adopts a μ_2-$\eta^1:\eta^1$-bridging (namely, one O of the carboxylate coordinates to Sb(III), the other coordinates to Sb(III) and Sm(III)). Each Sm(III) coordinates to four edta^{4-}, forming 2-D layers packed parallel to the *bc* plane (figure 3). The closest intra-chain Sb1···Sm, Sm···Sm and Sb1···Sb2 separations are 6.3092(10), 13.0096(18), and 12.5370(19) Å, respectively. Then, the 2-D sheets are further linked by μ_2-$\eta^1:\eta^1$-bridging carboxylates, resulting in a 3-D open framework with channels along the *a*-axis, and the uncoordinated water molecules and nitrate are trapped in channels of the 3-D framework (figure 4). The Sm–$O_{carboxylate}$ bonds formed between neighboring structural units play an important role in constructing the high-dimensional coordination polymer. Crystal structure of **1** is acentric with a 3-D framework. Figure 4 depicts the molecular packing arrangement in the unit cell along the *a*-axis.

3.2. *Thermal decomposition reactions of 1*

The thermal stability and decomposition patterns of **1** were investigated by the TG-DSC analysis. As shown in figure 5, the DSC curve shows two weak endothermic

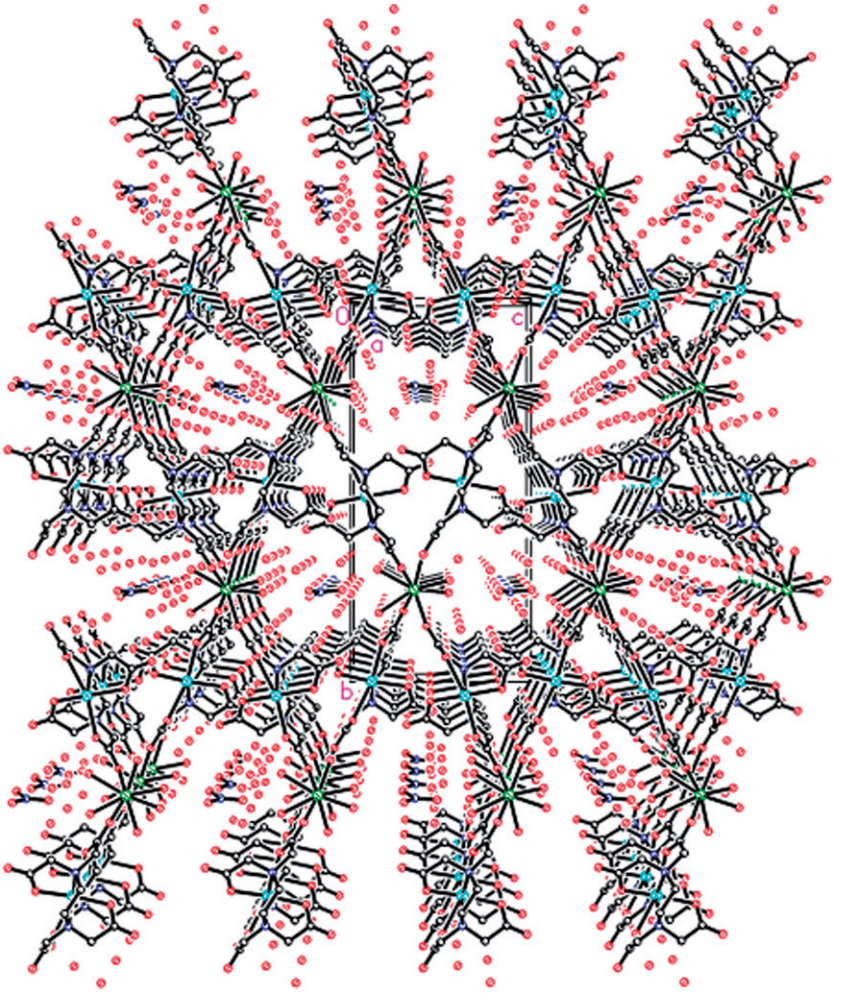

Figure 4. Packing diagram of **1** along the *a*-axis. All hydrogen atoms are omitted for clarity.

peaks between 30°C and 210°C, corresponding to the loss of free and coordinated water molecules (Exp. 11.27%; Calcd 11.63% for $7.55H_2O$) on **1**. From 210°C to 520°C, three discrete steps in the TG curve with three apparent exothermic peaks on DSC curve could be recognized due to the release of nitrate and the ligands. Between 210°C and 350°C, two $(CH_2)_2N(CH_2CO_2)$ groups with one NO_2 and CO_2 molecules are lost (Exp. 24.83%; Calcd 24.82%). The mass loss of 12.08% in the next step corresponds to the release of two $N(CH_2)_3$ and $3/4O_2$ (Calcd 11.64%) between 350°C and 410°C. The loss (12.98%) from 410°C to 520°C could be associated with the removal of the remaining five CO (Calcd 11.98% for 5CO). The eliminated CO can burn in air and release enormous heat. The heat of reaction is about $2150\,J\,g^{-1}$, giving an appreciable exothermic peak at 478°C in the DSC curve. The remaining mass stays almost constant until 1000°C; the residue of the thermal decomposition may be $1/2Sm_2O_3$ and Sb_2O_3. The theoretical total weight losses are calculated assuming that the residual oxide

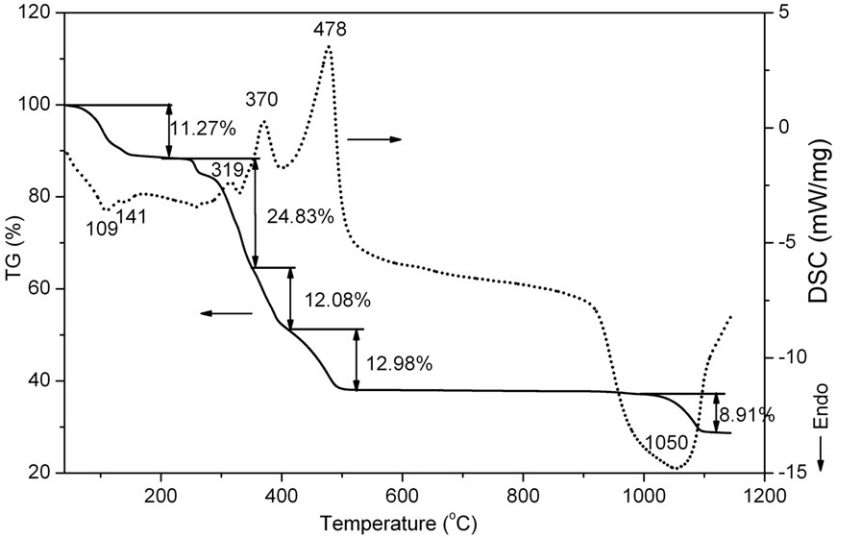

Figure 5. TGA and DSC curves of **1**.

corresponds to the stoichiometric formula Sb_2O_3 and $1/2Sm_2O_3$ (Exp. 38.84%; Calcd 39.93%). Some Sb_2O_3 will volatilize with increasing temperature, resulting in the loss of mass at 1050°C [27]. The final residue may be a mixture of antimony(III) and samarium(III) oxides.

3.3. *Fluorescence analysis of 1*

The solid-state luminescence of **1** was investigated at room temperature. Figure 6(a) shows that the excitation spectrum monitored at 595 nm emission consists of one broad excitation band at 200–270 nm, corresponding to the $^1S_0$–$^1P_1$ and $^1S_0$–$^3P_1$ transitions of the s^2 electron of Sb(III) [28, 29]. The characteristic f–f transition within the Sm(III) f^5 configuration at 330–500 nm is attributed to transitions from the $^6H_{5/2}$ ground state to the $^4K^4L_{17/2}$ (345 nm), $^4D_{15/2}$, $^6P_{15/2}$ (362 nm), $^4L_{17/2}$ (375 nm), $^4K_{11/2}$ (402 nm), $^4M_{19/2}$ (417 nm), $^4G_{9/2}$ (441 nm), $^5D_3$ (465 nm), and $^4I_{13/2}$ (478 nm) excited levels. Figure 6(b) shows one broad emission band from 200 to 500 nm. These emission bands arise from transition between $^3P_1$ and $^3P_1$ (excited states) to $^1S_0$ (ground state) of Sb(III) [30]. In figure 6(c), the emission spectrum of solid **1** consists of four main lines at 560 nm ($^4G_{5/2} \rightarrow {}^6H_{5/2}$), 595 nm ($^4G_{5/2} \rightarrow {}^6H_{7/2}$), 641 nm ($^4G_{5/2} \rightarrow {}^6H_{9/2}$), and 697 nm ($^4G_{5/2} \rightarrow {}^6H_{11/2}$) upon excitation at 400 nm. These emission bands were attributed to the $^4G_{5/2} \rightarrow {}^6H_J$ ($J = 5/2$, 7/2, 9/2 and 11/2) transitions of the Sm(III)-centered luminescence [31]. The Sb(III) emission band at wavelengths between 200 and 500 nm significantly overlaps with excitation bands of Sm(III) ions, which may result in energy transfer from the emission of Sb(III) to Sm(III). The Sb(III) is a sensitizer for luminescence of Sm(III) [32].

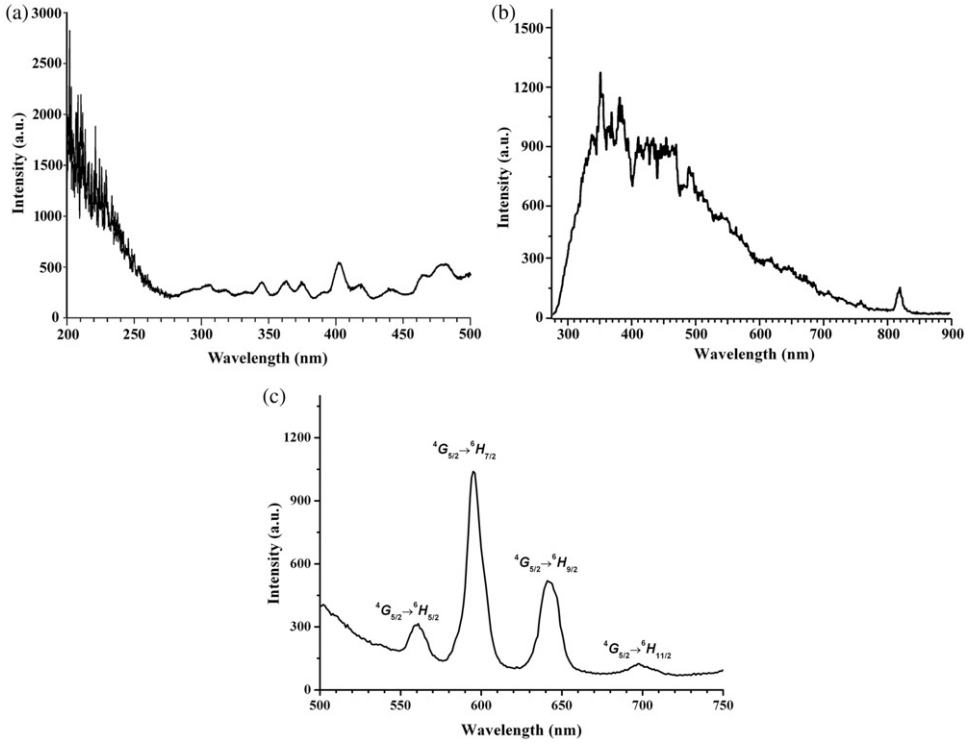

Figure 6. The excitation spectrum of **1** corresponding to 595 nm emission (a). The emission spectrum of **1** obtained after excitation at 220 nm (b) and 400 nm (c).

4. Conclusion

A new edta-linked trinuclear complex, **1**, has been synthesized, and characterized by EA, single-crystal X-ray diffraction analysis, FT-IR, and TG-DSC. Sb(III) is six coordinate by two nitrogen atoms and four oxygen atoms from one $edta^{4-}$. The center Sm(III) is eight coordinate by four oxygen atoms from H_2O and four carboxylate oxygen atoms from four $edta^{4-}$. Each $edta^{4-}$ links Sb(III) chains to make 2-D heterometallic sheets. The 2-D sheets are further linked by bridging carboxylates to generate a 3-D open framework structure. Thermal analyses show decomposition processes from 30°C to 1100°C of **1** and the final residue at 1100°C is mixed oxide compounds. The luminescence of **1** at room temperature suggests that **1** has the potential as a luminescent material.

Supplementary data

CCDC-795524 contains the supplementary crystallographic data for $C_{20}H_{39.11}N_5O_{26.55}Sb_2Sm$. These data can be obtained free of charge from The Cambridge

Crystallographic Data Center via Email: deposit@ccdc.cam.ac.uk or http://www.ccdc.cam.ac.uk/data_request/cif

Acknowledgments

This work was supported by the Open Project of State Key Laboratory Cultivation Base for Nonmetal Composites and Functional Materials (Grant Nos. 10zxfk18 and 10zxfk32) and the Southwest University of Science and Technology researching project (Grant No. 10zx7118).

References

[1] A.R. Ramya, M.L.P. Reddy, A.H. Cowley, K.V. Vasudevan. *Inorg. Chem.*, **49**, 2407 (2010).
[2] P.A. Tanner, C.-K. Duan. *Coord. Chem. Rev.*, **254**, 3026 (2010).
[3] M.V. Lucky, S. Sivakumar, M.L.P. Reddy, A.K. Paul, S. Natarajan. *Cryst. Growth Des.*, **11**, 857 (2011).
[4] J. Vallejo, I. Castro, J. Ferrando-Soria, M. del Pino Déniz-Hernández, C. Ruiz-Pérez, F. Lloret, M. Julve, R. Ruiz-García, J. Cano. *Inorg. Chem.*, **50**, 2073 (2011).
[5] T. Yamaguchi, J.-P. Costes, Y. Kishima, M. Kojima, Y. Sunatsuki, N. Bréfuel, J.-P. Tuchagues, L. Vendier, W. Wernsdorfer. *Inorg. Chem.*, **49**, 9125 (2010).
[6] N. Sakagami, Y. Yamada, T. Konno, K.-I. Okamoto. *Inorg. Chim. Acta*, **288**, 7 (1999).
[7] J.J. Borrás-Almenar, E. Coronado, D. Gatteschi, C. Zanchini. *Inorg. Chim. Acta*, **207**, 105 (1993).
[8] E. Coronado, M. Drillon, P.R. Nugteren, L.J. De Jongh, D. Beltran, R. Georges. *J. Am. Chem. Soc.*, **111**, 3874 (1989).
[9] F. Sapina, E. Coronado, D. Beltran, R. Burriel. *J. Am. Chem. Soc.*, **113**, 7940 (1991).
[10] Y. Tao, G. Song, L. Biaoguo. *Polyhedron*, **17**, 2243 (1998).
[11] M. Shimoi, Y. Orita, T. Uehiro, I. Kita, T. Iwamoto, A. Ouchi, Y. Yoshino. *Chem. Soc. Jpn.*, **53**, 3189 (1980).
[12] N.V. Sawant, J.B. Biswal, S.S. Garje. *J. Coord. Chem.*, **64**, 1758 (2011).
[13] D.C. Reis, M.C.X. Pinto, E.M. Souza-Fagundes, S.M.S.V. Wardell, J.L. Wardell, H. Beraldo. *Eur. J. Med. Chem.*, **45**, 3904 (2010).
[14] J. Duffin, B.G. Campling. *J. Hist. Med. Allied Sci.*, **57**, 61 (2002).
[15] P. Sharma, D. Perez, A. Cabrera, N. Rosas, J.L. Arias. *Acta Pharmacol. Sin.*, **29**, 881 (2008).
[16] E.R.T. Tiekink. *Crit. Rev. Oncol. Hemat.*, **42**, 217 (2002).
[17] G.M. Sheldrick. *SHELXS-97, Program for the Solution of Crystal Structures*, University of Göttingen, Germany (1997).
[18] G.M. Sheldrick. *SHELXL-97, Program for the Refinement of Crystal Structures*, University of Göttingen, Germany (1997).
[19] H.K. Fun, S. Shanmuga Sundara Raj, I.A. Razak, A.B. Ilyukhin, R.L. Davidovich, J.W. Huang, S.Z. Hu, S.W. Ng. *Acta Crystallogr. C*, **55**, 905 (1999).
[20] B. Marrot, C. Brouca-Cabarrecq, A. Mosset. *J. Chem. Crystallogr.*, **28**, 447 (1998).
[21] L.K. Templeton, D.H. Templeton, A. Zalkin, H.W. Ruben. *Acta Crystallogr. B*, **38**, 2155 (1982).
[22] M. Liang, Y.-Q. Sun, D.-Z. Liao, Z.-H. Jiang, S.-P. Yan, P. Cheng. *J. Coord. Chem.*, **57**, 275 (2004).
[23] Q. Yu, X. Zhou, M. Liu, J. Chen, Z. Zhou, X. Yin, Y. Cai. *J. Rare Earth*, **26**, 178 (2008).
[24] J. Wang, P. Hu, B. Liu, X. Jin, Y. Kong, J. Gao, D. Wang, B. Wang, R. Xu, X. Zhang. *J. Coord. Chem.*, **63**, 2193 (2010).
[25] J. Gao, D. Li, J. Wang, X. Jin, T. Wu, K. Li, P. Kang, X. Zhang. *J. Coord. Chem.*, **64**, 2234 (2011).
[26] T.-H. Zhou, F.-Y. Yi, P.-X. Li, J.-G. Mao. *Inorg. Chem.*, **49**, 905 (2010).
[27] G. Zhong, S. Luan, P. Wang, Y. Guo, Y. Chen, Y. Jia. *J. Therm. Anal. Calorim.*, **86**, 775 (2006).
[28] Z. Deng, F. Tang, D. Chen, X. Meng, L. Cao, B. Zou. *J. Phys. Chem. B*, **110**, 18225 (2006).
[29] B.S. Naidu, M. Pandey, V. Sudarsan, R.K. Vatsa, R. Tewari. *Chem. Phys. Lett.*, **474**, 180 (2009).
[30] E.W.J.L. Oomen, W.M.A. Smit, G. Blasse. *J. Phys. C: Solid State Phys.*, **19**, 3263 (1986).
[31] Y.-X. Chi, S.-Y. Niu, J. Jin. *Inorg. Chim. Acta*, **362**, 3821 (2009).
[32] G. Blasse, B.C. Grabmaier, *Luminescent Materials*, Springer, Berlin (1994).